

# RETRACTED ARTICLE: miR-31 Modulates Liver Cancer HepG2 Cell Apoptosis and Invasion via ROCK1/F-Actin Pathways

This article was published in the following Dove Press journal:  
*OncoTargets and Therapy*

Xin Zhang   
Lan Xu  
Ting Yang

Department of Laboratory, Cancer  
Hospital of China Medical University,  
Liaoning Cancer Hospital and Institute,  
Shenyang, Liaoning 110042, People's  
Republic of China

**Purpose:** Liver cancer is one of the most common malignant tumors in the world. miR-31 is downregulated in liver cancer and associated with tumor growth and metastasis. However, the underlying mechanism remains unclear.

**Methods:** Cellular apoptosis was detected via MT<sub>0</sub>-TUNEL assay, LDH release and Annexin V/PI flow-cytometry analysis. Cellular migration and invasion were measured by the Transwell chamber assay. Mitochondrial functions were evaluated via mitochondrial membrane potential JC-1 staining and mPTP opening assessment. The mitophagy activity was examined via Western blots.

**Results:** In the present study, our results confirm that miR-31 promotes apoptosis and inhibits proliferation and metastasis in liver cancer HepG2 cells. In vitro, miR-31 promotes HepG2 cell apoptosis through the mitochondrial pathway as indicated by mitochondrial potential reduction, increased mPTP opening, LDH release and imbalance of pro- and anti-apoptotic proteins. Furthermore, miR-31 reduces the energy generation by inhibiting mitochondrial respiratory function. At least, it is demonstrated that miR-31 triggers the mitochondrial damage via ROCK1/F-actin pathway. Inhibiting the ROCK1/F-actin pathway abolishes the effects of miR-31 mimic on mitochondrial injury, apoptosis, proliferation arrest and migration inhibition.

**Conclusion:** Our results reveal that miR-31 can inhibit HepG2 cell survival and metastasis by activating the ROCK1/F-actin pathway.

**Keywords:** miR-31, apoptosis, ROCK1, F-actin, mitochondrial

## Introduction

Liver cancer is the sixth most common malignant tumor around the world and the fourth leading cause of cancer death worldwide.<sup>1,2</sup> Hepatocellular carcinoma (HCC) is the main pathological type of liver cancer.<sup>3</sup> The main treatment methods for HCC include surgical treatment, arterial embolization, systemic chemotherapy and molecular targeted drug therapy.<sup>4</sup> However, due to the insidious onset, rapid progress and low early diagnosis rate of liver cancer, most patients are already in the advanced stage of the disease at the time of diagnosis, and the treatment effect is not good.<sup>5</sup> In advanced liver cancer cases, the 5 years' tumor recurrence and metastasis rate are as high as 40~70%.<sup>6</sup> Therefore, to explore the molecular biology process underlying liver cancer progression will help us better understand this disease and find effective targeted therapies.

As small non-coding RNAs, microRNAs (miRNAs) have been shown to contribute to regulate the translation of eukaryotic gene by altering mRNA expression and being

Correspondence: Xin Zhang  
Department of Laboratory, Cancer  
Hospital of China Medical University,  
Liaoning Cancer Hospital and Institute,  
No. 44 Xiaoheyan Road, Dadong District,  
Shenyang, Liaoning 110042, People's  
Republic of China  
Email: lnszlyjyjkzx@163.com

involved in cancer initiation and progression.<sup>7,8</sup> Recent works have reported that miR-31 is downregulated in liver cancers when compared to normal tissue and its overexpression is related to liver cancer cell lines HepG2 viability and metastasis.<sup>9,10</sup> However, the underlying mechanism is still enigmatic.

As the energy house in eukaryotic cells, it is reported that mitochondria play a critical role in cancer initiation and progression, including non-small-cell lung, prostate<sup>11,12</sup> and breast cancer.<sup>13</sup> The impaired mitochondrial homeostasis results in mitochondrial potential collapse, ATP undersupply and mPTP opening, and subsequently inhibits cellular survival, proliferation and metastasis.<sup>14,15</sup> Moreover, a recent study has suggested that mitochondria is significant in drug resistance through a closer connection with rough the endoplasmic reticulum (ER) in liver cancer compared with other tumor cells.<sup>16</sup> These findings indicate that the special role of mitochondria in liver cancer cells. However, whether miR-31 inhibits liver cancer HepG2 cell survival and metastasis through mitochondrial has yet to be fully elucidated.

Rho-associated coiled-coil containing protein kinase 1 (ROCK1)/F-actin pathway functions as a tumor suppressor in several types of cancer.<sup>17,18</sup> Activating ROCK1/F-actin pathway suppressed cell survival and migration in non-small cell lung cancer (NSCLC) A549 cells.<sup>19</sup> Moreover, increased evidence have revealed the relationship between mitochondrial and ROCK1/F-actin pathway.<sup>20,21</sup> In cerebral ischemia-reperfusion injury, ROCK1/F-actin is involved in Drp1-related mitochondrial fission and followed cellular apoptosis.<sup>22</sup> However, whether miR-31 affects liver cancer HepG2 cell survival and metastasis through the ROCK1/F-actin pathway remains uncertain. Thus, this study aims to explore mechanisms of miR-31 induced tumor suppression with a focus on mitochondrial injury and the ROCK1/F-actin pathway.

## Materials and Methods

### Cell Culture

The liver cancer cell lines, HepG2, and normal live cell lines, L02, were obtained from the American Type Culture Collection (Manassas, VA, USA). All cell lines were grown in RPMI-1640 supplied with 10% FBS and 1% penicillin–streptomycin under a humidified 5% CO<sub>2</sub>-enriched at atmosphere at 37°C. To inhibit ROCK1 activity, Y-27632 (5 mM; cat. no. S1049; Selleck Chemicals, Houston, TX, USA) was added to the medium for 4 h.<sup>19</sup>

To activate mitophagy, FCCP (5 μM, cat. no. S1049; Selleck Chemicals, Houston, TX, USA) was used 2 h before treatment.<sup>23</sup>

### Quantitative Real-Time PCR (qRT-PCR)

qRT-PCR was performed according to the manufacturer's instructions.<sup>24</sup> Briefly, total RNA was extracted from the cells using TRIzol reagent (Invitrogen; Thermo Fisher Scientific, Inc., Carlsbad, CA, USA) and reverse transcribed with a TaqMan MicroRNA Reverse Transcription kit (Takara Bio, Inc., Otsu, Japan) at 37°C for 30 min according to the manufacturer's instructions. qPCR was performed using the SYBR Green RT-PCR kit (Takara Bio, Inc.). The following primers were used for polymerase chain reaction: Cytokeratin, forward, TAAATCAGTACGCTGAGGGG, reverse, TCCGCTGGTGAACCAGGCTT; E-cadherin, forward, TCCATCTCTGGTCTACGCC, reverse, TCTTCAGGCACTCTGTTT; Vimentin, forward, GCGTCGCTACCTTCGTGAAT, reverse, TCAATGTCACTGGCCATCTAA; N-cadherin, forward, GTGCCCTAGCCAAGGGAATTCAGC, reverse, GCGTTCTGTCCACTCAGGAGG; GAPDH, forward, ACCCATCTCTCCACCTTGA, reversed, CTGTTGCTGTAGCCAAATTC, miR-31, forward 5'-UAGCAGCACAGAAATCTGGC-3', reverse 5'-CAUAUUUCUGUGCUGCAUU-3'; U6, forward 5'-CTCGCTTCGGCAGCACA-3', reverse 5'-AACGCTTCACGAATTTGCGT-3'. The thermocycling conditions were as follows: 95°C for 5 min, followed by 40 cycles at 95°C for 40 s, 60°C for 30 s and 72°C for 30 s. U6 and GAPDH were selected as internal controls for micro (mi)RNA and mRNA, respectively.<sup>25</sup> Fold-changes for mRNA expressions were calculated using the 2<sup>-ΔΔCq</sup> method.<sup>26</sup>

### Western Blotting

Samples were lysed by RIPA buffer supplemented with PMSF. Bicinchoninic acid protein assay was used to detect the protein concentration. The antibodies used in the present were as follows: cyclin D1 (1:1000; cat. no. ab16663; Abcam), cyclin E (1:1000; cat. no. ab33911; Abcam), cyt-c (1:1000; cat. no. ab90529; Abcam), ROCK1 (1:1000; cat. no. ab45171; Abcam), Caspase-9 (1:1000; cat. no. ab32539; Abcam), cleaved caspase-3 (1:1000; cat. no. ab49822; Abcam), F-actin (1:1000; cat. no. ab205; Abcam), B-cell lymphoma 2 (Bcl2; 1:1000; cat. no. 3498; Cell Signaling Technology, Inc., Shanghai, China), Bcl2-associated death promoter (Bad; 1:1000; cat. no. 9292; Cell Signaling Technology, Inc., Shanghai, China). The blots were detected

with an enhanced chemiluminescence substrate kit (Thermo Fisher Scientific, Inc.), and band intensity levels were analyzed using Quantity One 4.6 software (Bio-Rad Laboratories, Inc.).

## Cellular Migration and Invasion

After treatment, HepG2 cell migration was analyzed using a Transwell chamber assay (24 wells, 8- $\mu$ m pore size with a polycarbonate membrane) as previously described.<sup>27</sup> Briefly, cells were suspended in serum-free medium and seeded into upper chambers that were either uncoated (for migration assay) or coated (for invasion assay) with BD Matrigel TM Basement Membrane Matrix. A volume of 0.5 mL of 20% FBS medium was added to the lower Transwell chamber as a chemoattractant. After incubation for 24 hrs, cells were fixed in 4% paraformaldehyde and stained with 0.1% Crystal Violet Staining Solution.

## 5-Ethynyl-2'-Deoxyuridine (EdU) Incorporation Assay

The EdU incorporation assay was performed using an EdU kit (cat. no. A10044; Thermo Fisher Scientific Inc.). After treatment, the cells ( $1 \times 10^6$ ) were incubated with the EdU (2 nM/well) for 2 h at 37°C. After washing with PBS for three times, the cells were fixed with 4% paraformaldehyde for 10 min at 37°C and were incubated with Apollo Staining reaction liquid for 30 min. DAPI was used to counterstain the nuclei for 15 min at room temperature under dilution at 37°C.

## Luciferase Activity Assay

Wild-type ROCK1 3'UTR (WT) and mutant ROCK1 3'UTR (MUT) containing the relative binding site of miR-31 were chemically synthesized and cloned downstream of the firefly luciferase gene in a pGL3-promoter vector (Ambion; Thermo Fisher Scientific, Inc.). HepG2 cells were placed on a 48-well plate and cultures until 80% confluence. Cells were then co-transfected with luciferase plasmids (2.5  $\mu$ g per  $3.5 \times 10^4$  cells/well) and miR-31 or control miRNA under DMEM medium supplemented with 10% fetal bovine serum (Gibco, Thermo Fisher Scientific, Inc.) using Lipofectamine 2000 (Thermo Fisher Scientific, Inc.) according to the manufacturer's protocol. At 48 h after transfection, the firefly and Renilla luciferase activities (Promega Corporation, cat. 117 no. E2810) were measured with a Dual-Luciferase Reporter Assay System (Promega Corporation, Madison, WI, USA).

## TUNEL, MTT and LDH Release Assay

A one-step TUNEL kit (Beyotime Institute of Biotechnology, Haimen, China) was used for TUNEL staining as previously described.<sup>28</sup> After the treatment, HepG2 cells were incubated with fluorescein-dUTP (Invitrogen; Thermo Fisher Scientific, Inc.) to stain apoptotic cell nuclei and DAPI (5mg/mL) to stain all cell nuclei at room temperature for 3 min. The slides were imaged under a confocal microscope at least 5 random separate fields. LDH release was measured using an LDH release kit (Beyotime, Beijing, China). The 3-(4,5-dimethylthiazol-2-yl)-2,5-diphenyltetrazolium bromide (MTT) assay was used to measure cell viability as previously described.<sup>29</sup>

## Annexin V/PI Flow-Cytometry Analysis

Cellular apoptosis was also detected quantitatively using the FITC Annexin V Apoptosis Detection Kit (556547, BD Bioscience).<sup>30</sup> The cells were stained with 5  $\mu$ L of FITC Annexin V and PI and incubated for 15 min at RT (25°C) in the dark. The stained cells were subsequently analyzed using a BD FACS-Calibur cytometer (BD Bioscience).

## ATP Generation, Mitochondrial Potential ( $\Delta\Psi$ m) and mPTP Opening

ATP generation was measured by a luciferase-based ATP assay kit (CellTiter-Glo<sup>®</sup> Luminescent Cell Viability Assay; cat. no. G7570; Promega Corporation, Madison, WI, USA) was according to the manufacturer's protocols. The  $\Delta\Psi$ m was visualized using the JC-1 Kit (Beyotime, China). Red fluorescence indicated normal mitochondrial potential, whereas green fluorescence indicated damage mitochondrial potential. The mPTP opening was assessed as the rapid dissipation of tetramethylrhodamine ethyl ester (TMRE) fluorescence. TMRE fluorescence was alternately excited at the wavelengths of 550 nm and 575 nm.<sup>31</sup>

## Isolation of Mitochondria-Enriched Fraction

Mitochondrial and cytoplasmic cyt-c expression was measured via isolation of the mitochondrial-enriched fraction, followed by Western blotting. Briefly, cells were washed with cold PBS and were scraped; the homogenates were then centrifuged at  $800 \times g$  for 5 min at 4°C. The supernatants were centrifuged at  $10,000 \times g$  for 20 min at 4°C to acquire pellets, which were spun again. The final pellets were suspended in lysis buffer (cat. no. P0013E; Beyotime

Institute of Biotechnology) containing 1% Triton X-100 and were noted as mitochondrial-rich lysate fractions.<sup>32</sup>

## Immunofluorescence Assay

We used immunofluorescence staining to determine F-actin. Briefly, cells were fixed by 4% paraformaldehyde for 10 min at room temperature. Following blocking with 5% bovine serum albumin (Sigma-Aldrich; Merck KGaA, Shanghai, China) in PBS for 1 h at room temperature, the cells were incubated with primary antibodies for 4 h at room temperature. Images were captured using a laser confocal microscope (TCS SP5; Leica Microsystems, Inc., Buffalo Grove, IL, USA). The primary antibody used was F-actin (1:500, Abcam, #ab205). DAPI (5 mg/mL; Sigma-Aldrich; Merck KGaA) was used to stain the nucleus at room temperature for 10 min.

## Transfection

The miR-31 mimic (miR-31-5p, miR-31 mimic group), miR-control (NC group) were purchased from GenePharma Company (Shanghai, China). HepG2 cells were transfected with 20 nM miR-31 mimic and miR-control with Lipofectamine 2000 (Invitrogen, Carlsbad, CA) according to the manufacturer's instruction. Transfection was performed for 48 h.

## Electron Transport Chain Complex (ETC<sub>x</sub>) Activity Detection

Complex I, II, and V activity was measured according to previous studies.<sup>33</sup> Mitochondrial respiratory function was measured polarographically at 30°C using a Biological Oxygen Monitor System (Hansatech Instruments, King's Lynn, UK) and a Clark-type oxygen electrode (Hansatech DW1, Norfolk, UK). Mitochondrial respiration was initiated by adding glutamate/malate to a final concentration of 5 and 0.5 mmol/L, respectively.

## Statistical Analysis

All analyses were performed with SPSS 20.0 software (IBM Corp., Armonk, NY, USA). The data are presented as the mean  $\pm$  standard deviation and statistical significance for each variable was estimated by a one-way analysis of variance followed by Tukey's test for the post hoc analysis.  $P < 0.05$  was considered to indicate a statistically significant difference. All experiments were repeated three times.

## Results

### miR-31 Enhances HepG2 Cell Apoptosis

Initially, the expression of miR-31 in the HepG2 cells and L02 cells was detected by qRT-PCR. Compared with L02 cells, the expression of miR-31 was reduced in the HepG2 cells (Figure 1A). To explore the role of miR-31 in the biological functions of HepG2 cells, a mimic of miR-31 was used in HepG2 cells to increase the expression of miR-31 (Figure 1B). Following the transfection of miR-31, cellular viability and apoptosis were measured. As indicated in Figure 1B, miR-31 mimic significantly reduced HepG2 cell viability compared with that of control groups. In agreement with these results, the cellular apoptotic rate, as evidenced by MT assay (Figure 1C), LDH release (Figure 1D), TUNEL<sup>+</sup> cells (Figure 1E and F) and Annexin V<sup>+</sup> cells (Figure 1G and H), was increased in response to miR-31 transfection compared with control group. It is concluded that miR-31 may act as a pro-apoptotic factor in HepG2 cells.

### Transfection of miR-31 Inhibits HepG2 Cell Proliferation and Metastasis

We further assessed the effects of miR-31 on cellular proliferation and metastasis. First, we used Western blotting assay to measure the expression of cyclin D1 and cyclin E, which could accelerate the cellular transition from the G0/G1 to S stage. As shown in Figure 2A–C, cyclin D1 and cyclin E expression were dramatically decreased in miR-31 transfected HepG2 cells compared with that in the control group. To provide more evidence, we also used EdU staining to figure out the function of miR-31 on HepG2 cell proliferation (Figure 2D and E). In miR-31 transfected HepG2 cells, the number of EdU-positive cells was significantly decreased compared with the control group. These results suggested that miR-31 is involved in the regulation of HepG2 cell proliferation.

Cellular migration and invasion are key determinants of malignant progression and metastasis.<sup>23</sup> Through transwell assay, we found that the migratory and invasive ability of HepG2 cells were decreased when responding to miR-31 mimic compared with the control group (Figure 2F–H). We also detected the expression of classical epithelial–mesenchymal transition (EMT) markers, including cytokeratin, E-cadherin, N-cadherin, and vimentin by qRT-PCR. As shown in Figure 2I–L, the mRNA levels of cytokeratin and E-cadherin were dramatically elevated, while mRNA levels of N-cadherin and vimentin



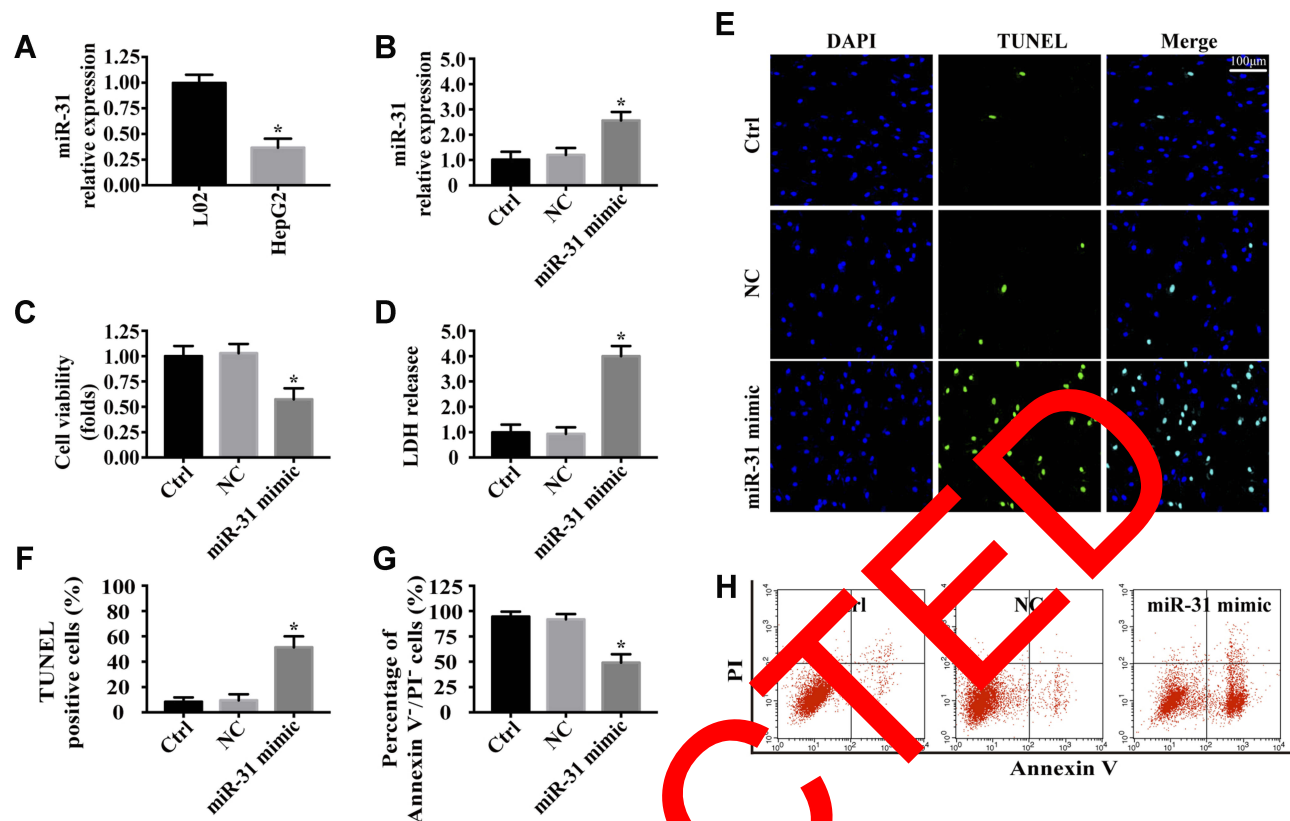


**Figure 1** miR-31 transfection activates HepG2 cell apoptosis.

**Notes:** (A) The expression of miR-31 in L02 and HepG2 cells. (B) The expression of miR-31 was measured by qRT-PCR. MTT assay (C) and LDH release (D) were performed in HepG2 cells following miR-31 mimics transduction. TUNEL staining (E–F) and Annexin V/PI flow-cytometry analysis (G–H) were used to detect the HepG2 cell viability. \*P < 0.05 vs the ctrl group or L02 group.

were significantly decreased in reaction to up-regulated miR-31, thus indicating that miR-31 suppressed HepG2 cell migration. In conclusion, all these results demonstrated that miR-31 affects HepG2 cell proliferation and metastasis.

## Transfection of miR-31 Activates Mitochondrial Apoptotic Pathway in HepG2 Cells

Previous studies have argued that mitochondrial dysfunction contributed to the regulation of cellular apoptosis, proliferation and migration.<sup>32</sup> To discover the underlying mechanism by which miR-31 induced HepG2 cell apoptosis, we focused on the mitochondrial related apoptosis pathway via the analysis of mitochondrial potential, its related apoptotic proteins, mPTP opening, cyt-c leakage and mitochondrial related apoptotic proteins. First, we used JC-1 staining to detect the mitochondrial potential (Figure 3A and B). Compared with the control group, the mitochondrial potential was observably decreased in

miR-31 transfected HepG2 cells as shown by the decreased red fluorescence and increased green ones. miR-31 mimic also enhanced the mPTP opening time (Figure 3C). In comparison with the control group, the transfection of miR-31 caused more cyt-c leakage from mitochondria into the cytoplasm (Figure 3D–F). Furthermore, proteins associated with mitochondrial damage were evaluated by Western blot (Figure 3G–K). Introduction of miR-31 increased the expression of pro-apoptotic proteins (Bax, caspase9 and caspase3) but decreased the anti-apoptotic proteins (Bcl-2 and x-IAP) compared with the control group. Collectively, all findings point out that miR-31 may activate the mitochondrial apoptotic pathway.

## miR-31 Contributes to Mitochondrial Dysfunction in HepG2 Cells

Mitochondria, the energy house of cell, is vital in the growth and metastasis of tumor cells.<sup>34,35</sup> Thus, we were concerned with the question whether miR-31 contributed

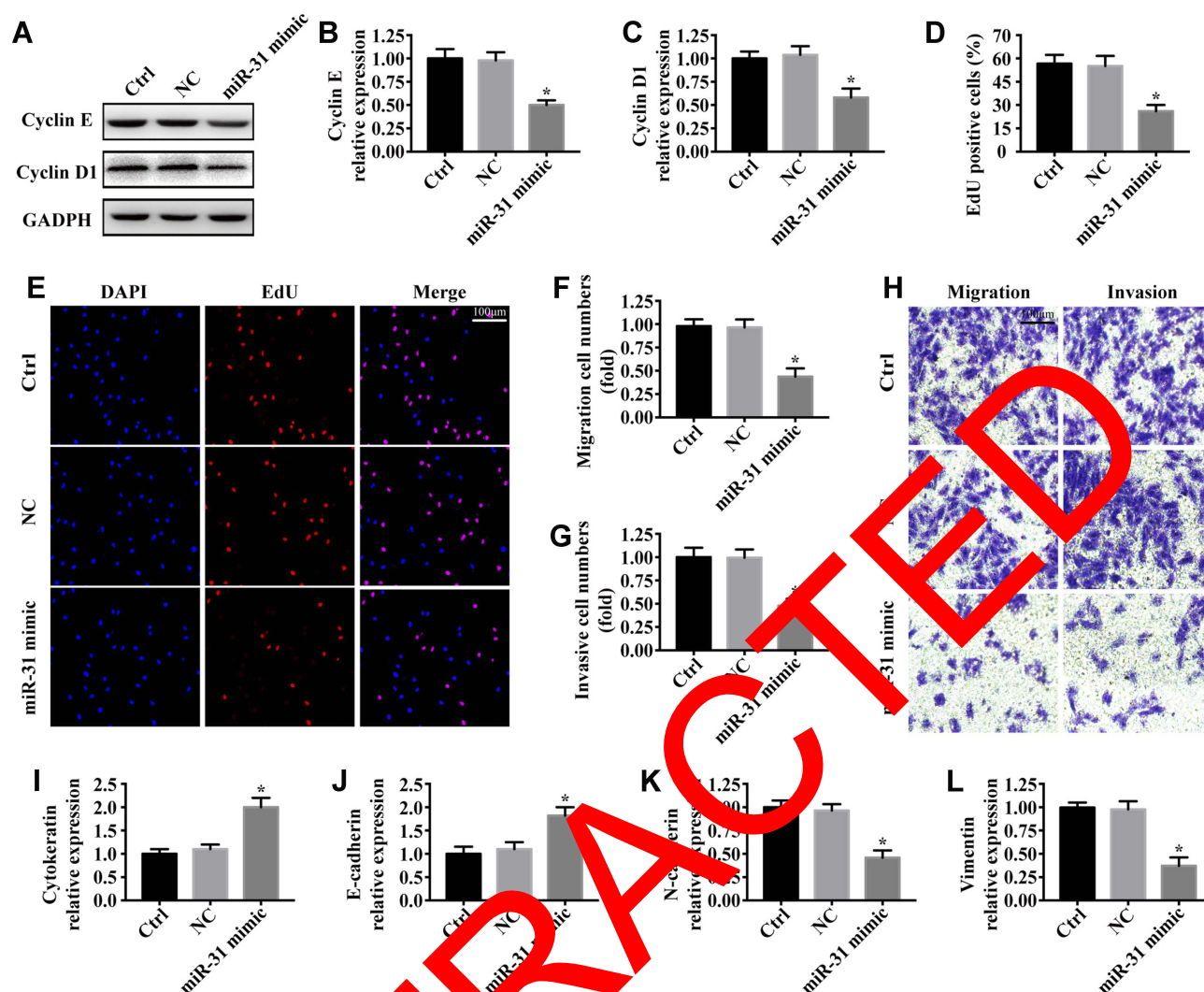


**Figure 2** miR-31 affects HepG2 cell proliferation and metastasis.

**Notes:** (A–C) Expression levels of proliferation-associated proteins were analyzed by Western blotting in HepG2 cells following miR-31 mimics transduction. (D–E) Cell proliferation was measured via EdU staining. (F–H) The migration and invasion assay were measured in HepG2 cells following miR-31 mimics transduction. (I–L) The mRNA levels of cytokerin, E-cadherin, N-cadherin, and vimentin were detected by qRT-PCR. \*P < 0.05 vs the ctrl group.

to mitochondrial dysfunction in HepG2 cells. To get a certain answer, we also investigated the role of miR-31 in mitochondrial metabolism in the present study. It was observed that miR-31 mimic inhibited the ATP generation in HepG2 cells compared to the control and NC group (Figure 4A). Moreover, miR-31 transfection decreased the activity of mitochondrial respiratory complexes, which were coupled to the decrease of the state 3 respiratory rate (Figure 4B–H). The current study also analyzed glucose uptake, lactate content, and the oxygen consumption rate in HepG2 cells after transfection of miR-31 (Figure 4I–K). As shown in Figure 4I–K, miR-31 mimic decreased glucose uptake and lactate product and oxygen consumption in HepG2 cells compared with the control

and NC group. Together, these results confirmed miR-31 contributed to the mitochondrial dysfunction in HepG2 cells.

### miR-31 Activates HepG2 cell Injury via ROCK1/F-Actin Pathways

Several researches have been said that ROCK1/F-actin pathways contributed to the mitochondrial related cell apoptosis, migration inhibition, and proliferation arrest in several cancer cells.<sup>36,37</sup> Thus, a question was raised whether miR-31 functions in HepG2 cells through ROCK1/F-actin pathways. To answer it, Y-27632, the inhibitor of ROCK1, was used in HepG2 cells transfected with miR-31 mimic. As shown in Figure 5A–C, the

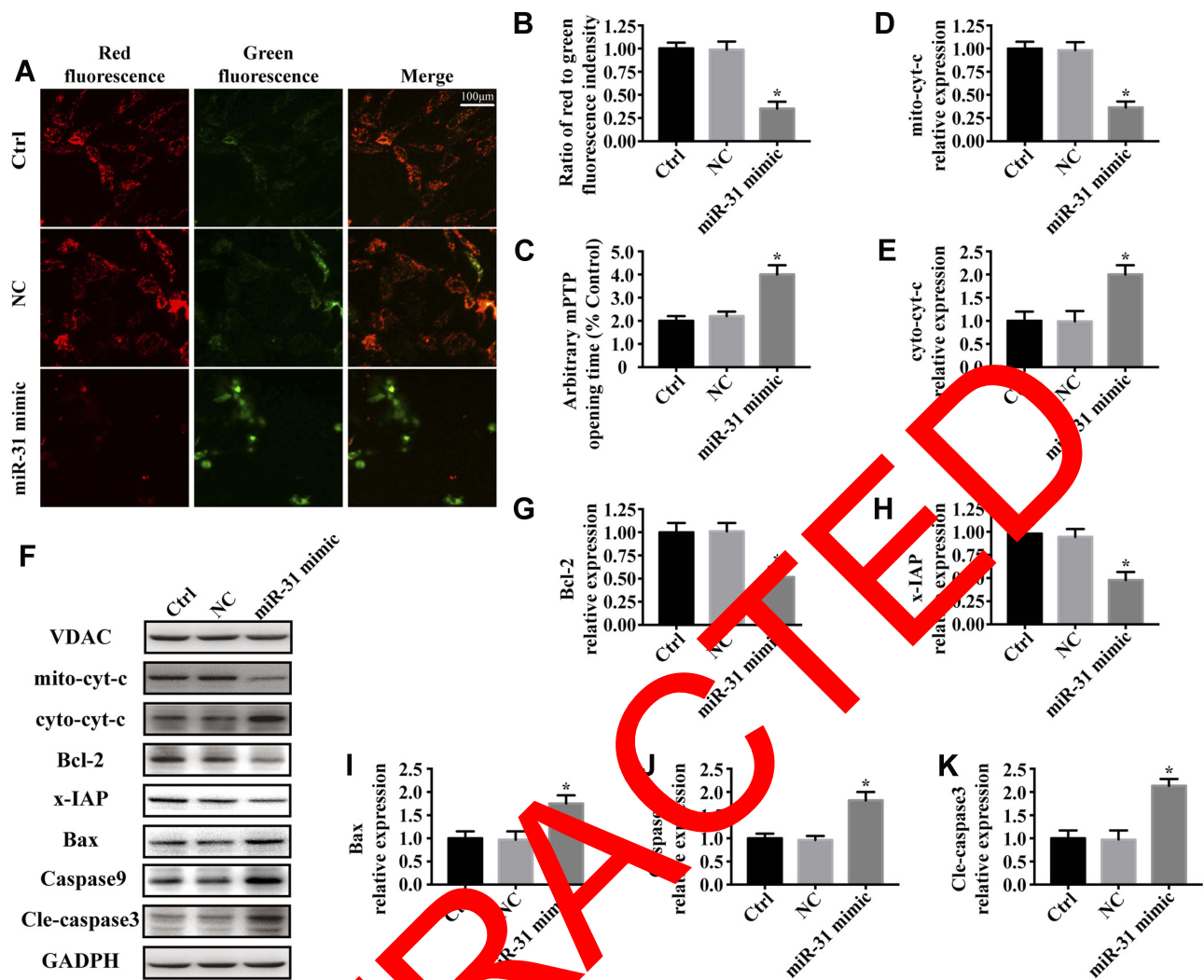


**Figure 3** miR-31 is associated with mitochondrial damage.

**Notes:** (A–B) The mitochondrial potential was measured by JC-1 assay. Red fluorescence indicated normal mitochondrial potential, whereas green fluorescence indicated damage mitochondrial potential. (C) miR-31 mimic promoted mPTP opening time in HEPG2 cells. (D–K) Western blotting was used to determine the protein level of mito-cyt-c, cyto-cyt-c, Bcl-2, x-IAP, Bax, Caspase9, and Cle-caspase3 in response to miR-31 transfection in HepG2 cells. \*P < 0.05 vs the ctrl group.

protein levels of ROCK1 were upregulated in response to miR-31 mimic, whereas F-actin expression was reduced. Y-27632 administration abolished the effect of miR-31 on ROCK1 and F-actin. Altogether, it implies that miR-31 can activate ROCK1/F-actin pathways.

Y-27632 also enhanced ATP generation (Figure 5D), maintained the mitochondrial potential (Figure 5E and F), and reduced the number of TUNEL positive cell (Figure 5G) in HepG2 cells followed miR-31 mimic. Furthermore, inhibiting ROCK1 reduced miR-31 mimic induced proliferation arrest as well as migration inhibition as evidenced by increased EdU positive cells (Figure 5H), migrated cells (Figure 5I and J) and longer filopodia (Figure 5K and L) outside of the cellular membrane. In one word, it signifies that ROCK1/F-actin pathways are necessary for

miR-31-mediated apoptosis, energy disorder, migration inhibition, and proliferation arrest.

Furthermore, qPCR analysis showed a 6-nt match to the miR-31 seed region with the 3'UTR of ROCK1 (Figure 5M). To test whether miR-31 directly targeted the 3'UTR of Mfn2, luciferase assays were performed using 3'UTR sequence fragments containing the predicted target of ROCK1 and its mutated version inserted downstream of a luciferase reporter (Figure 5N). The results demonstrated that the luciferase activity was downregulated in cells co-transfected with miR-31 mimics and the wild-type ROCK1 3'UTR compared with the mutated type, suggesting that ROCK1 is a target gene of miR-31. These data indicate that miR-31 directly regulates transcription and expression of ROCK1.

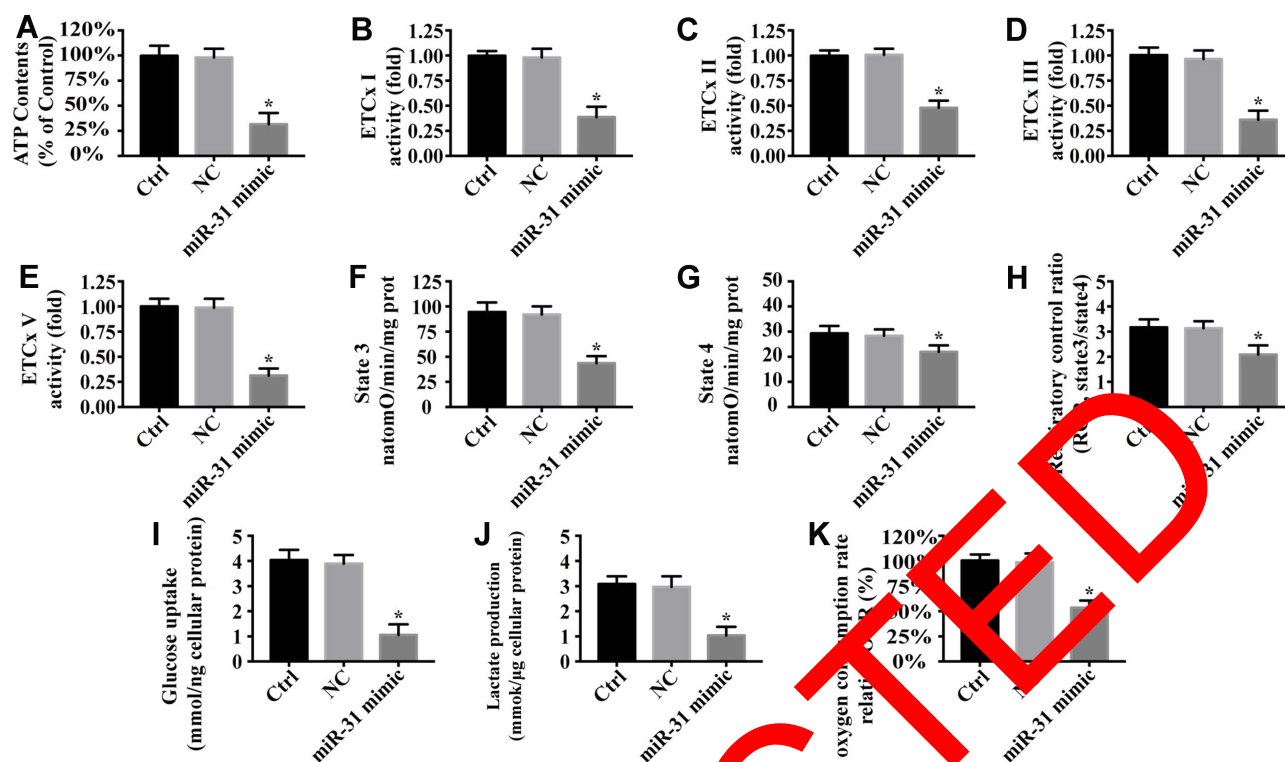


**Figure 4** The effects of miR-31 on mitochondrial respiratory function in HepG2 cells.

**Notes:** (A) ATP generation was measured following miR-31 transfection in HepG2 cells. (B–E) Mitochondrial respiratory complex protein activity was evaluated via ELISA analyses. miR-31 inhibited mitochondrial respiratory. (F–H) Effect of miR-31 on state 3 respiration, state 4 respiration, respiratory control ratio (RCR [state 3/state 4]). (I–K) Glucose uptake, lactate production, and oxygen consumption were measured following miR-31 mimic transfection. \*P < 0.05 vs the ctrl group.

## Discussion

Numerous studies have revealed that miRNAs are intimately related to tumor initiation and progression.<sup>38,39</sup> Previous works have confirmed that miR-31 is downregulated in liver cancer and involved in liver cancer cell apoptosis, migration impairment, and proliferation delay.<sup>10,40</sup> But the underlying mechanisms remain unclear. The present study fills this gap and confirmed that miR-31 promotes HepG2 cells mitochondria-related apoptosis and inhibits proliferation and metastasis by activating the ROCK1/F-actin pathway.

Over the past decades, the part of mitochondrial homeostasis in tumor growth and metastasis has received increasing attention.<sup>41</sup> Compared with normal cells, cancer cells have faster growth and invasive abilities requiring more energy from the mitochondria.<sup>42,43</sup> Through interacting with the endoplasmic reticulum (ER), mitochondria is also involved in the regulation of sphingolipid metabolism which is strongly associated with cell proliferation, metastasis, and drug resistance.<sup>44,45</sup> In addition, mitochondrial fission and mitophagy are also reported to promote cancer cell death.<sup>46</sup> Mitochondrial Reactive Oxygen Species

(mROS) also can activate several oncogenic signaling pathways, such as Ras/MAPK/ERK, PI3K/Akt, and IKK/KF-B.<sup>47</sup> All the above works have shown a critical part that the mitochondria plays a role in the development of cancer. This study demonstrates that miR-31 induces mitochondrial injury and inhibits HepG2 cell survival, proliferation, and metastasis consistent with a previous study.

F-actin has been proved to be involved in the regulation, cell proliferation, and movement. In the process of mitochondrial fission, F-actin is rearranged on the mitochondrial outer membrane surface and forms a ring structure with Drp1.<sup>48</sup> Moreover, F-actin exacerbates astrocyte apoptosis via activating the Ras2-cAMP-PKA pathway.<sup>49</sup> Notably, F-actin homeostasis is regulated by ROCK1, which depolymerizes F-actin into G-actin. Besides, ROCK1 is strongly associated with cancer growth and metastasis. At the molecular level, ROCK1 promotes mitochondrial dysfunction and mitochondria-related apoptosis through the PTEN pathway and PI3K/Akt pathway in human leukemia cells.<sup>50</sup> In this study, we can be certain that miR-31 is the upstream effector of ROCK1/F-actin axis, and inhibiting the ROCK1/F-actin pathway abolishes



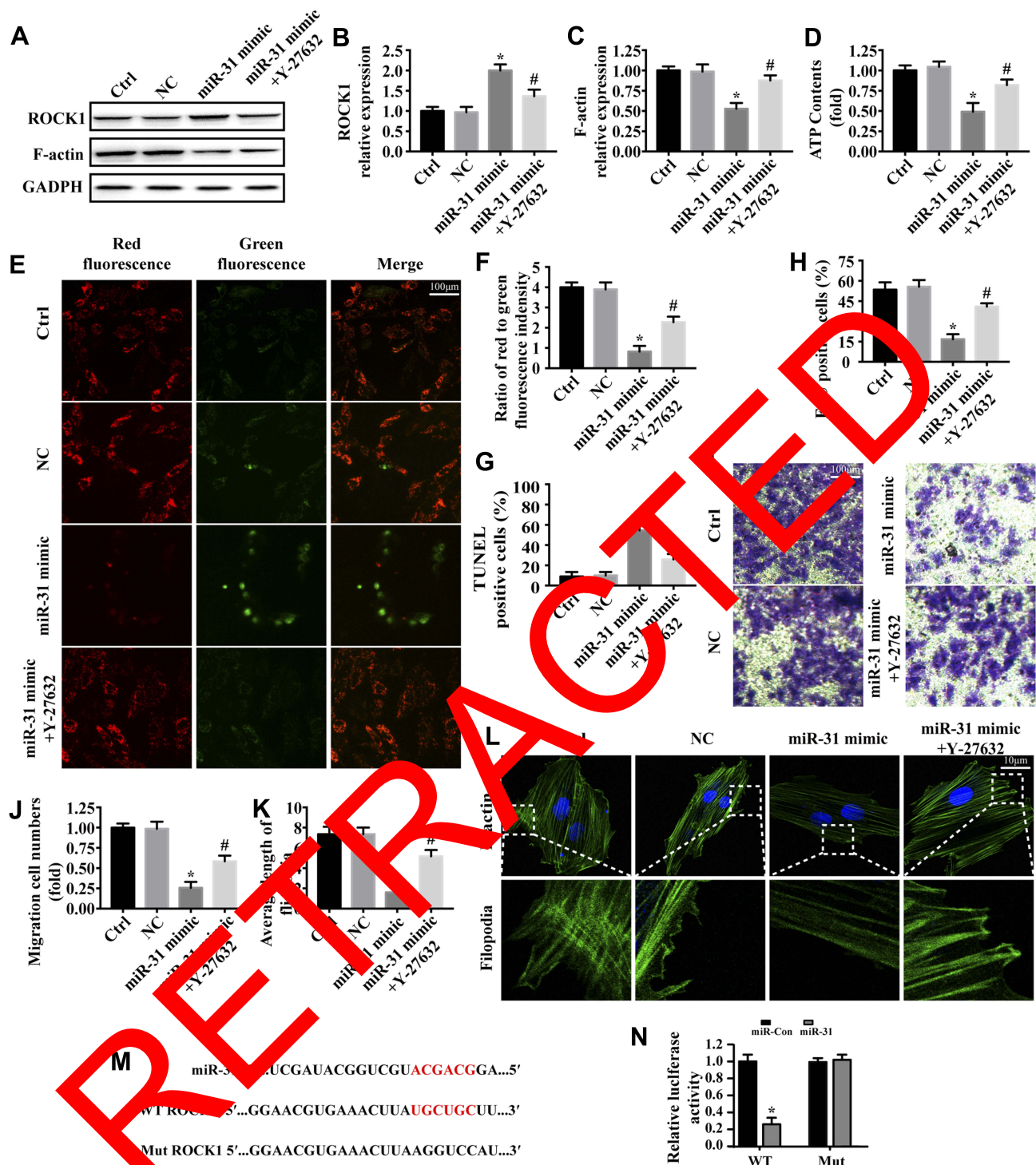


**Figure 5** miR-31 inhibits HepG2 cell proliferation and metastasis and promotes apoptosis via activating ROCK1/F-actin pathways.

**Notes:** (A–C) The protein level of ROCK1 and F-actin was measured by Western blotting. The ROCK1/F-actin pathway was activated in HepG2 cells in response to miR-31 mimic. (D–F) The effects of ROCK1/F-actin on ATP generation and mitochondrial potential. (G–H) Inhibiting the ROCK1/F-actin pathway reduced miR-31 induced apoptosis and proliferation arrest. (I–J) The effects of ROCK1/F-actin on cellular migration. (K–L) The average length of filopodia was measured in response to miR-31 transduction and Y-27632 treatment. (M) Computational analysis was performed for miRNA seed sequences complementary to the 3'UTR of ROCK1 mRNA. (N) Luciferase assay for post-transcriptional repression of ROCK1. \*P < 0.05 vs the ctrl group. #P < 0.05 vs the miR-31 mimic group.

the beneficial effects of miR-31 on viability, mitochondrial function, proliferation, and movement in liver cancer HepG2 cells. However, the targets of miR-31 are not

clearly described in this study. The underlying mechanism by which miR-31 increased ROCK1 expression should be measured in the future study. ROCK1/F-actin is reported

to promote mitochondrial dysfunction and apoptosis via activating mitochondrial fission.<sup>20,22</sup> Whether mitochondrial fission is involved in miR-31 induced mitochondrial injury and apoptosis in HepG2 cells needs further research.

To explore the role of ROCK1/F-actin pathways in miR-31 induced HepG2 cells mitochondrial dysfunction and apoptosis. Y-27632, the inhibitor of ROCK1, was used in HepG2 cells transfected with miR-31 mimic. It is worth noting that some studies had shown that Y-27632 only inhibits its activity, usually has no effect on its expression.<sup>51,52</sup> However, other studies have shown that Y-27632 inhibits ROCK1 through inhibiting its expression.<sup>26,53</sup> The different effects of Y-27632 on ROCK1 may be related to cell types.

## Limitation

Recent works have reported that the liver cancer cell lines (HepG2) exhibited relatively low miR-31 expression levels compared to the non-cancer cell line, L02.<sup>9,10</sup> Thus, the effect of miR-31 in normal cell line was not detected in this study, and this is a limitation of this study.

## Conclusions

Altogether, our data explain the underlying mechanism of miR-31 induce apoptosis, proliferation arrest and movement inhibition with a focus on ROCK1/F-actin pathway and mitochondrial injury in liver cancer HepG2 cells. Our findings shed new light into an understanding of liver cancer development and progression and may provide a new therapeutic approach for liver cancer.

## Data Sharing Statement

The datasets used and/or analyzed during the current study are available from the corresponding author on reasonable request.

## Author Contributions

All authors made substantial contributions to conception and design, acquisition of data, or analysis and interpretation of data; took part in drafting the article or revising it critically for important intellectual content; gave final approval of the version to be published; and agree to be accountable for all aspects of the work.

## Disclosure

The authors report no conflicts of interest in this work.

## References

- Wallace MC, Preen D, Jeffrey GP, Adams LA. The evolving epidemiology of hepatocellular carcinoma: a global perspective. *Expert Rev Gastroenterol Hepatol*. 2015;9(6):765–779. doi:10.1586/1747-4124.2015.1028363
- Zhang X, Li J, Shen F, Lau WY. Significance of presence of microvascular invasion in specimens obtained after surgical treatment of hepatocellular carcinoma. *J Gastroenterol Hepatol*. 2018;33(2):347–354. doi:10.1111/jgh.2018.33.issue-2
- Wang J, Lu L, Luo Z, et al. miR-383 inhibits cell growth and promotes cell apoptosis in hepatocellular carcinoma by targeting IL-17 via STAT3 signaling pathway. *Biomed Pharmacother*. 2019;120:109551. doi:10.1016/j.biopha.2019.109551
- Sim HW, Knox J. Hepatocellular carcinoma in the era of immunotherapy. *Curr Probl Cancer*. 2018;42(1):40–53. doi:10.1016/j.cup.2017.10.007
- Jiang JF, Lao YC, Yuan BH, et al. Treatment of hepatocellular carcinoma with portal vein tumor thrombus: advances and challenges. *Oncotarget*. 2017;8(20):33921–33921. doi:10.18632/oncotarget.15411
- Pinyol R, Llovet JM. Hepatocellular carcinoma: genome-scale metabolic models for hepatocellular carcinoma. *Nat Rev Gastroenterol Hepatol*. 2014;10(6):336–337. doi:10.1038/nrgastro.2014.70
- Bartel DP. MicroRNAs: target recognition and regulatory functions. *Cell*. 2009;136(2):281–297. doi:10.1016/j.cell.2009.01.002
- Shukla GC, Singh J, Bhat S. MicroRNAs: processing, maturation, target recognition and regulatory functions. *Mol Cell Pharmacol*. 2011;3(3):83–92.
- Gao G, Han C, Zhang Z, Wang L, Xu J. Increased expression of microRNA-31-5p inhibits cell proliferation, migration, and invasion via upregulating Smad transcription factor in HepG2 hepatocellular carcinoma cell line. *Biochem Biophys Res Commun*. 2017;490(2):371–377. doi:10.1016/j.bbrc.2017.06.050
- Tian C, Rao S, Liu L, et al. Klf4 inhibits tumor growth and metastasis by targeting microRNA-31 in human hepatocellular carcinoma. *Int J Mol Med*. 2017;39(1):47–56. doi:10.3892/ijmm.2016.2812
- Wu X, He Y, Zhang G, et al. Royleanone diterpenoid exhibits potent anticancer effects in LNCaP human prostate carcinoma cells by inducing mitochondrial mediated apoptosis, cell cycle arrest, suppression of cell migration and downregulation of mTOR/PI3K/AKT signalling pathway. *J BUON*. 2018;23(4):1055–1060.
- Lee YJ, Oh JE, Lee SH. Arctigenin shows preferential cytotoxicity to acidity-tolerant prostate carcinoma PC-3 cells through ROS-mediated mitochondrial damage and the inhibition of PI3K/Akt/mTOR pathway. *Biochem Biophys Res Commun*. 2018;505:1244–1250. doi:10.1016/j.bbrc.2018.10.045
- Liang X, Xu SM, Zhang J, Li J, Shen Q. Cascade amplifiers of Intracellular ROS based on mitochondria-targeted core-shell ZnO-TPP@D/H nanorods for breast cancer therapy. *ACS Appl Mater Interfaces*. 2018. doi:10.1021/acsami.8b12590
- Lee KM, Giltman JM, Balko JM, et al. MYC and MCL1 cooperatively promote chemotherapy-resistant breast cancer stem cells via regulation of mitochondrial oxidative phosphorylation. *Cell Metab*. 2017;26(4):633–647. doi:10.1016/j.cmet.2017.09.009
- Zacksenhaus E, Shrestha M, Liu JC, et al. Mitochondrial OXPHOS induced by RB1 deficiency in breast cancer: implications for anabolic metabolism, stemness, and metastasis. *Trends Cancer*. 2017;3(11):768–779. doi:10.1016/j.trecan.2017.09.002
- Yeh TC, Chiang PC, Li TK, et al. Genistein induces apoptosis in human hepatocellular carcinomas via interaction of endoplasmic reticulum stress and mitochondrial insult. *Biochem Pharmacol*. 2007;73(6):782–792. doi:10.1016/j.bcp.2006.11.027
- Liang H, Zhang C, Guan H, Liu J, Cui Y. LncRNA DANCER promotes cervical cancer progression by upregulating ROCK1 via sponging miR-335-5p. *J Cell Physiol*. 2018;234:7266–7278.

18. Kreutzman A, Colom-Fernandez B, Jimenez AM, et al. Dasatinib reversibly disrupts endothelial vascular integrity by increasing non-muscle myosin II contractility in a ROCK-dependent manner. *Clin Cancer Res*. 2017;23(21):6697–6707. doi:10.1158/1078-0432.CCR-16-0667
19. Zhang W, Liu K, Pei Y, Ma J, Tan J, Zhao J. Mst1 regulates non-small cell lung cancer A549 cell apoptosis by inducing mitochondrial damage via ROCK1/F-actin pathways. *Int J Oncol*. 2018. doi:10.3892/ijo.2018.4586
20. Li GB, Cheng Q, Liu L, et al. Mitochondrial translocation of cofilin is required for allyl isothiocyanate-mediated cell death via ROCK1/PTEN/PI3K signaling pathway. *Cell Commun Signal*. 2013;11:50. doi:10.1186/1478-811X-11-50
21. Yin M, Lu Q, Liu X, Wang T, Liu Y, Chen L. Silencing Drp1 inhibits glioma cells proliferation and invasion by RHOA/ROCK1 pathway. *Biochem Biophys Res Commun*. 2016;478(2):663–668. doi:10.1016/j.bbrc.2016.08.003
22. Geng C, Wei J, Wu C. Yap-Hippo pathway regulates cerebral hypoxia-reoxygenation injury in neuroblastoma N2a cells via inhibiting ROCK1/F-actin/mitochondrial fission pathways. *Acta Neurol Belg*. 2018. doi:10.1007/s13760-018-0944-6
23. Shi C, Cai Y, Li Y, et al. Yap promotes hepatocellular carcinoma metastasis and mobilization via governing cofilin/F-actin/lamellipodium axis by regulation of JNK/Bnip3/SERCA/CaMKII pathways. *Redox Biol*. 2018;14:59–71. doi:10.1016/j.redox.2017.08.013
24. Liu C, Zhang H, Liu H. Long noncoding RNA UCA1 accelerates nasopharyngeal carcinoma cell progression by modulating miR-124-3p/ITGB1 axis. *Oncotargets Ther*. 2019;12:8455–8466. doi:10.2147/OTT.S215819
25. Shuang Y, Li C, Zhou X, Huang Y, Zhang L. MicroRNA-195 inhibits growth and invasion of laryngeal carcinoma cells by directly targeting DCUN1D1. *Oncol Rep*. 2017;38(4):2155–2165. doi:10.3892/or.2017.5875
26. Livak KJ, Schmittgen TD. Analysis of relative gene expression data using real-time quantitative PCR and the 2<sup>-ΔΔC<sub>T</sub></sup> (ΔΔC<sub>T</sub>) Method. *Methods*. 2001;25(4):402–408. doi:10.1006/meth.2001.1212
27. Zhou H, Zhu P, Guo J, et al. Ripk3 induces mitochondrial apoptosis via inhibition of FUNDC1 mitophagy in cardiac IR. *Redox Biol*. 2017;13:498–507. doi:10.1016/j.redox.2017.07.007
28. Zhou L, Cha G, Chen L, Yang C, Li D, Ge M. HIF1α/PD-L1 axis mediates hypoxia-induced cell apoptosis and tumor progression in follicular thyroid carcinoma. *Oncotargets Ther*. 2019;12:6461–6470. doi:10.2147/OTT.S2019.12.6461
29. Zhou H, Zhang Y, Hu S, et al. Melatonin protects cardiac microvasculature against ischemia/reperfusion injury via suppression of mitochondrial fission-VDAC1-HK2-mPTP-mitophagy axis. *J Pineal Res*. 2017;63(1).
30. Wang M, Tian Z, Zhu J, et al. Sichong formula inhibits the proliferation and metastasis of human gastric cancer cells. *Oncotargets Ther*. 2019;12:5741–5750. doi:10.2147/OTT.S199605
31. Zhu J, Hu S, Jin Q, et al. Ripk3 promotes ER stress-induced necroptosis in cardiac injury: a mechanism involving calcium overload/XO/ROS/mPTP pathway. *Redox Biol*. 2018;16:157–168. doi:10.1016/j.redox.2018.02.019
32. Jin Q, Li R, Hu S, et al. DUSP1 alleviates cardiac ischemia/reperfusion injury by suppressing the Mff-required mitochondrial fission and Bnip3-related mitophagy via the JNK pathways. *Redox Biol*. 2018;14:576–587. doi:10.1016/j.redox.2017.11.004
33. Zhou H, Hu S, Jin Q, et al. Mff-dependent mitochondrial fission contributes to the pathogenesis of cardiac microvasculature ischemia/reperfusion injury via induction of mROS-mediated cardiolipin oxidation and HK2/VDAC1 disassociation-involved mPTP opening. *J Pineal Res*. 2017;63(3).
34. Ni K, Lan G, Veroneau SS, Duan X, Song Y, Lin W. Nanoscale metal-organic frameworks for mitochondria-targeted radiotherapy-radiodynamic therapy. *Nat Commun*. 2018;9(1):4321. doi:10.1038/s41467-018-06655-7
35. Mori K, Uchida T, Yoshie T, et al. A mitochondrial ROS pathway controls matrix metalloproteinase 9 levels and invasive properties in RAS-activated cancer cells. *FEBS J*. 2018;286:459–478.
36. Liu Y, Wang Y, Fu X, Lu Z. Long non-coding RNA NEAT1 promoted ovarian cancer cells' metastasis through regulation of miR-382-3p/ROCK1 axis. *Cancer Sci*. 2018;109(7):2188–2198. doi:10.1111/cas.13647
37. Lin L, Li M, Lin L, Xu X, Jiang G, Wu L. FPPS mediates TGF-beta1-induced non-small cell lung cancer cell invasion and the EMT process via the RhoA/Rock1 pathway. *Biochem Biophys Res Commun*. 2018;496(2):536–541. doi:10.1016/j.bbrc.2018.01.066
38. Wen J, Hu Y, Liu Q, et al. miR-424 coordinates multi-layered regulation of cell cycle progression to promote esophageal squamous cell carcinoma cell proliferation. *EBioMedicine*. 2018;37:110–121. doi:10.1016/j.ebiom.2018.10.043
39. Wu Q, Sun S, Li Z, et al. Tumour-oncogene exosomal miR-155 triggers cancer-associated cachexia to promote tumour progression. *Mol Cancer*. 2018;17(1):15. doi:10.1186/s12943-018-0899-5
40. Du Z, Niu S, Gu X, Xu J. MicroRNA-141-NDRG3 regulation axes are essential for hepatocellular carcinoma survival and drug resistance. *Cancer Biomarkers*. 2017;19(2):217–230. doi:10.3233/CBM-170568
41. Wallace DC. Mitochondria and cancer. *Nat Rev Cancer*. 2012;12(7):685–698. doi:10.1038/nrc3365
42. Zong WX, Rabinowitz JD. Mitochondria WE. *Cancer. Mol Cell*. 2016;61(5):667–676. doi:10.1016/j.molcel.2016.02.011
43. Rauckhorst J, Taylor EB. Mitochondrial pyruvate carrier function and cancer metabolism. *Curr Opin Genet Dev*. 2016;38:102–109. doi:10.1016/j.cde.2016.05.003
44. Annunziata I, Sano R, d'Azzo A. Mitochondria-associated ER membranes (MAMs) and lysosomal storage diseases. *Cell Death Dis*. 2018;9(3):328. doi:10.1038/s41419-017-0025-4
45. Boppana NB, Stochaj U, Kodiha M, et al. Enhanced killing of SCC17B human head and neck squamous cell carcinoma cells after photodynamic therapy plus fenretinide via the de novo sphingolipid biosynthesis pathway and apoptosis. *Int J Oncol*. 2015;46(5):2003–2010. doi:10.3892/ijo.2015.2909
46. Greene AW, Grenier K, Aguilera MA, et al. Mitochondrial processing peptidase regulates PINK1 processing, import and Parkin recruitment. *EMBO Rep*. 2012;13(4):378–385. doi:10.1038/embor.2012.14
47. Liou GY, Storz P. Reactive oxygen species in cancer. *Free Radic Res*. 2010;44(5):479–496. doi:10.3109/10715761003667554
48. Zhou H, Hu S, Jin Q, et al. Mff-dependent mitochondrial fission contributes to the pathogenesis of cardiac microvasculature ischemia/reperfusion injury via induction of mROS-mediated cardiolipin oxidation and HK2/VDAC1 disassociation-involved mPTP opening. *J Am Heart Assoc*. 2017;6(3). doi:10.1161/JAHA.116.005328
49. Zhu K, He Q, Li L, Zhao Y, Zhao J. Silencing thioredoxin1 exacerbates damage of astrocytes exposed to OGD/R by aggravating apoptosis through the Actin-Ras2-cAMP-PKA pathway. *Int J Neurosci*. 2018;128(6):512–519. doi:10.1080/00207454.2017.1398159
50. Zhang R, Li G, Zhang Q, et al. Hirsutidine induces mPTP-dependent apoptosis through ROCK1/PTEN/PI3K/GSK3β pathway in human lung cancer cells. *Cell Death Dis*. 2018;9(6):598. doi:10.1038/s41419-018-0641-7
51. Wang Y, Shou Z, Fan H, et al. Protective effects of oxymatrine against DSS-induced acute intestinal inflammation in mice via blocking the RhoA/ROCK signaling pathway. *Biosci Rep*. 2019;39(7). doi:10.1042/BSR20182297

52. Robertson-Gray OJ, Walsh SK, Ryberg E, Jonsson-Rylander AC, Lipina C, Wainwright CL. 1-alpha-Lysophosphatidylinositol (LPI) aggravates myocardial ischemia/reperfusion injury via a GPR55/ROCK-dependent pathway. *Pharmacol Res Perspect*. 2019;7(3):e00487. doi:10.1002/prp2.487
53. Liu WY, Tang Q, Zhang Q, et al. Lycorine induces mitochondria-dependent apoptosis in hepatoblastoma HepG2 cells through ROCK1 activation. *Front Pharmacol*. 2019;10:651. doi:10.3389/fphar.2019.00651

RETRACTED

### OncoTargets and Therapy

Dovepress

### Publish your work in this journal

OncoTargets and Therapy is an international, peer-reviewed, open access journal focusing on the pathological basis of all cancers, potential targets for therapy and treatment protocols employed to improve the management of cancer patients. The journal also focuses on the impact of management programs and new therapeutic

agents and protocols on patient perspectives such as quality of life, adherence and satisfaction. The manuscript management system is completely online and includes a very quick and fair peer-review system, which is all easy to use. Visit <http://www.dovepress.com/testimonials.php> to read real quotes from published authors.

Submit your manuscript here: <https://www.dovepress.com/oncotargets-and-therapy-journal>